ACS chemical biology

pubs.acs.org/acschemicalbiology

Article

Development of a Versatile Plant-Derived Mitochondrial Targeting Sequence Based on a Reporter Protein Sorting Analysis and Biological Information

Naoya Abe, Masaki Odahara, Shamitha Rao Morey, and Keiji Numata*

Cite This: *ACS Chem. Biol.* 2024, 19, 2515−2524

Read Online

ACCESS | Metrics & More | Article Recommendations | Supporting Information

ABSTRACT: Methods for the delivery of exogenous substances to specific organelles are important because each organelle functions according to its own role. Specifically, mitochondria play an important role in energy production. Recently, plant mitochondrial transformation via delivery methods to mitochondria has been actively researched. Mitochondrial targeting sequences (MTSs) are essential for transporting bioactive molecules, such as nucleic acids, to mitochondria. However, the selectivity and efficacy of MTSs as carrier molecules in plants are not yet sufficient. In this study, we developed an effective MTS in plants via a quantitative comparison of the targeting functions of several MTSs. The presequence of HSP60 from *Nicotiana tabacum*, which is highly similar to that of several other model plants, showed high mitochondrial-targeting ability among the MTSs tested. This result suggests the applicability of the HSP60 presequence for MTSs in various plants. We further investigated this HSP60 presequence through stepwise shortening on the basis of secondary structure prediction, aiming to simplify synthesis and increase the solubility of the peptides. As shown by assessment of the mitochondrial targeting ability, the 15 residues from the N-terminus of the HSP60 presequence for the MTS, which is particularly conserved among various model plants, retained a targeting efficacy comparable to that of the full-length HSP60 presequence. This developed sequence from the HSP60 sequence is a promising MTS for transfection into plant mitochondria.

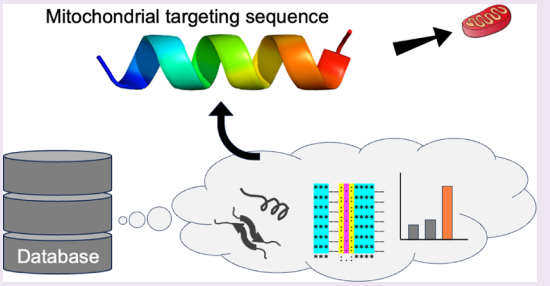

INTRODUCTION

Owing to the population explosion and drastic climate change, it is assumed that food supplies will not meet the demand for food in the near future.[1−3] The expansion of farmland damages forests, contributing to environmental degradation and climate change.[4] Agricultural productivity should increase to maintain the sustainability of agriculture.[5] To improve the productive efficacy of agriculture, researchers have made advances in genetic engineering.[6−8] Genetic modification is an effective way to develop a new productive variety. The genomic transformation of the nucleus and chloroplasts has been accomplished, but mitochondrial transformation is a challenge because conventional methods for genomic transformation cannot be used. Mitochondria and chloroplasts have genomes different from those of the nucleus does. Mitochondria play an important role in energy production.[9] Through the transformation of the mitochondrial genome, the development of highly productive plants is expected. Additionally, plant mitochondria contain a cytoplasmic male sterility-related gene.[10] Controlling the cytoplasmic male sterility is important in plant breeding. Furthermore, a previous report showed that resistance to highly saline environments is increased by the overexpression of manganese superoxide dismutase in *Arabidopsis thaliana* mitochondria.[11] Plant mitochondrial transformation is expected to increase the productivity in agriculture.

Mitochondria have their own genomes, but most mitochondrial proteins are encoded in the nucleus as precursors. In the mitochondrial protein precursors, a presequence is tagged at the N-terminus of the mitochondrial protein for mitochondria targeting.[12] These presequences have been utilized as mitochondrial targeting sequences (MTSs). The MTS in the N-terminus guides the precursor to the mitochondria and is recognized by the translocator of the outer mitochondrial membrane (TOM).[13] After the TOM is reached, the precursor with the MTS is incorporated into the mitochondrial matrix.[14] Generally, MTSs have an N-terminal import domain and a C-terminal processing domain.[15] The import domain plays a critical role in targeting mitochondria, and the processing domain contributes to recognition by the mitochondrial processing peptidase in the mitochondrial matrix. When the N-terminal domain of the presequence is removed, the

Received: September 17, 2024
Revised: October 18, 2024
Accepted: October 30, 2024
Published: December 2, 2024

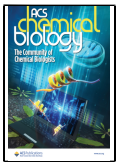

https://doi.org/10.1021/acschembio.4c00625
ACS Chem. Biol. 2024, 19, 2515−2524

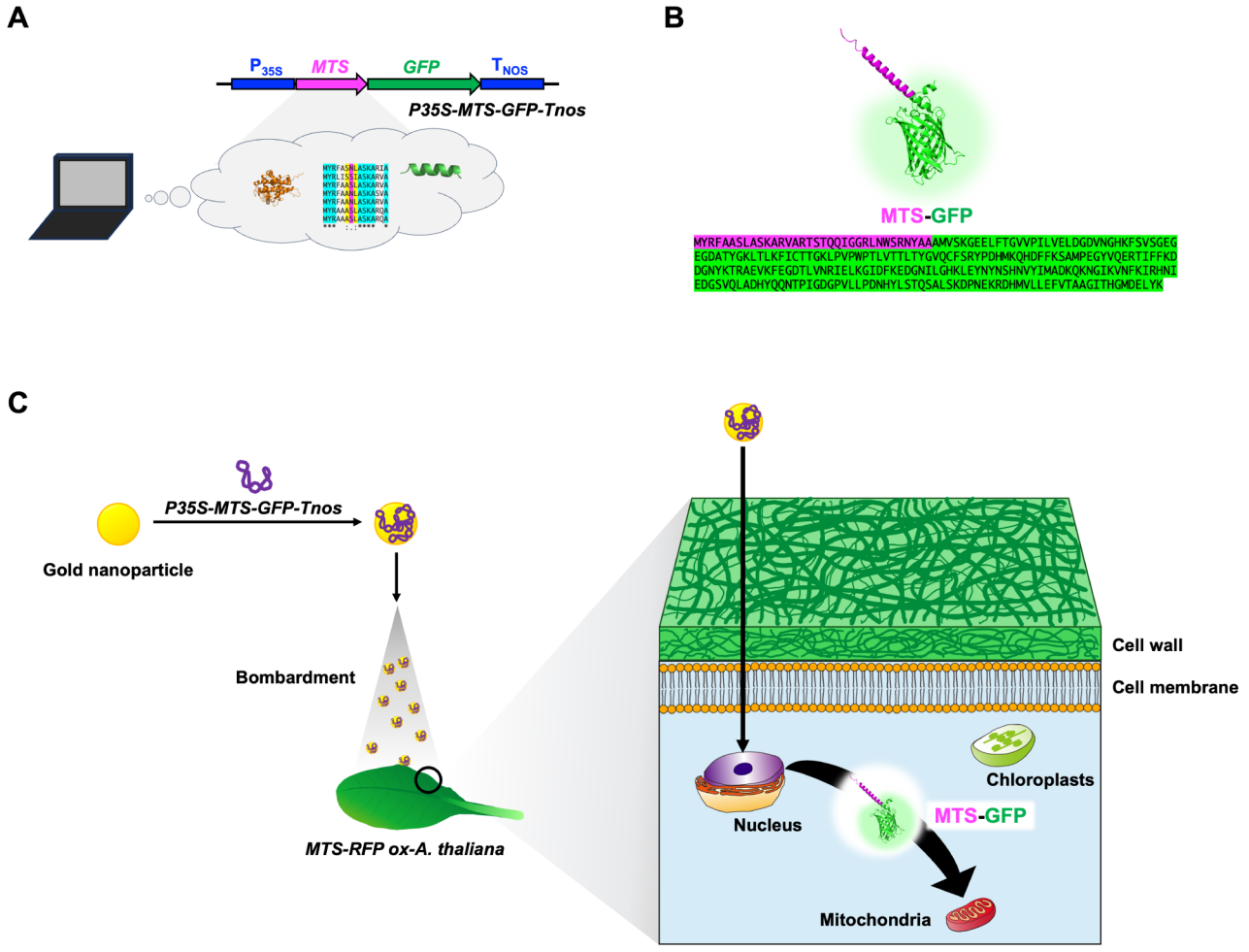

Figure 1. Conceptual diagram of this work. (A) Construction of the *P35S-MTS-GFP-Tnos* plasmid. The MTS was designed based on biological information. (B) The structure and sequence of MTS-modified green fluorescent protein (GFP). The MTS was fused to the N-terminus of GFP. (C) Schematic illustration of MTS-GFP expression and localization in an epidermal cell of an MTS-RFP ox-*A. thaliana* leaf. *P35S-MTS-GFP-Tnos* was designed for MTS-GFP expression in the cytosol. When the MTS is effective, MTS-GFP is delivered to the mitochondria. The mitochondrial-targeting functions of several MTSs were compared on the basis of the colocalization of MTS-GFP and mitochondria.

function of the target is impaired.[16] In contrast, the deletion of the C-terminal domain does not affect import.[17] The MTS is cleaved from the precursor in the mitochondrial matrix. The specificity of MTSs is not very high, and MTSs differ between proteins or species. MTSs are composed mainly of polar, hydrophobic, and cationic amino acids.[15] Furthermore, the sequences form a helical structure.[18] The TOM recognizes the characteristic amino acids and the secondary structure of MTSs.

Fusion peptide methods using MTS have led to gene delivery to mitochondria instead of particle bombardment methods, which are available for the transformation of nuclei and chloroplasts. In the particle bombardment method, gold nanoparticles coated with DNA are introduced into the nuclei or chloroplasts without targeting. However, DNA cannot be delivered to mitochondria via particle bombardment methods because mitochondria are smaller and more dynamic than nuclei and chloroplasts are. Therefore, mitochondrial targeting is important for the delivery of genes to mitochondria. In fusion peptide methods, the modification of peptide/DNA complexes with MTS allows mitochondrial targeting of DNA.[19−23] For gene delivery to plant mitochondria, Cytcox12 (MLSLRQSIRFFK) has been utilized mainly as an MTS.[19,21,23,24] Cytcox12 comprises 12 amino acids and was shortened from the presequence of cytochrome C oxidase subunit IV.[25] The cytochrome C oxidase subunit IV is from *Saccharomyces cerevisiae*. Most presequences have approximately 30 amino acid residues. The shortened sequences from the presequences are generally used as the MTS for transfection, because presequences are too long to synthesize. A gene carrier modified with Cytcox12 was successfully transfected into plant mitochondria. However, the mitochondrial selectivity of Cytcox12-modified carriers is not high.[23,24] As a result, the transfection efficacy was not sufficient to produce a stable mitochondrial mutant. The development of more efficient MTSs for plants is needed to increase the mitochondrial transfection efficacy.

In this study, the mitochondrial-targeting ability of several presequences in intact plants was quantitatively compared (Figure 1). The candidate MTSs were designed with biological information (Figure 1A). Among them, the most effective sequence was chosen and optimized by secondary structure prediction, solubility, and reporter protein sorting (Figure 1B, part C). In particular, the N-terminal 15 amino acids of the heat shock protein 60 (HSP60) presequence from *Nicotiana tabacum* (N15) showed high mitochondrial targeting function

https://doi.org/10.1021/acschembio.4c00625
ACS Chem. Biol. 2024, 19, 2515−2524

Table 1. MTSs used in this Experiment[a]

MTS	Organism	Sequence	Prediction score
Cytcox12	*S. cerevisiae*	MLSLRQSIRFFK	0.6919
Cytcox25	*S. cerevisiae*	MLSLRQSIRFFKPATRTLCSSRYLL	0.7204
SD3	*A. thaliana*	MMMMNLLRRSAIAIGRQSKSKLASFSSATQPCSGIPKSSKRVFSNSFLSKD	0.7201
HSP60	*N. tabacum*	MYRFAASLASKARVARTSTQQIGGRLNWSRNYAA	0.6847

[a]The sequences from the N-terminus to the alanine of the 9th residue, to the serine of the 10th residue, to the lysine of the 11th residue, to the alanine of the 15th residue, and the glutamine of the 20th residue were called N9, N10, N11, N15, and N20, respectively. N34 is the full length of the HSP60 presequence. The predicted probability for the mitochondrial targeting peptide is displayed as a prediction score

in these candidate sequences. This N-terminal 15 amino acid sequence is well conserved in several model plants. These results indicate that N15 has the potential to be an effective MTS in many plants. The N15 sequence contributes not only to transfection but also to various studies on plant mitochondria.

RESULTS AND DISCUSSION

MTSs. We chose the following 4 types of MTSs to evaluate their mitochondrial targeting efficacy (Table 1). Cytcox12 comprises 12 amino acid residues and has been commonly used for the transfection of plant mitochondria.[25] Cytcox25 is a full-length presequence of cytochrome *c* oxidase subunit IV from *S. cerevisiae*.[26] Cytcox12 is a shortened sequence from Cytcox25. SD3 is a probable translocase of inner mitochondrial membrane 21 (TIM21) in *A. thaliana*.[27] HSP60 is a chaperonin located in mitochondria.[28] In this study, we used the N-terminal presequences of SD3 from *A. thaliana* and HSP60 from *N. tabacum* for MTSs. The probability of the MTS was predicted via TargetP-2.0.[29] The prediction score indicates how likely the sequence is to be an MTS. The prediction score for the MTSs did not differ significantly across sequences.

Quantification of Mitochondrial Targeting Efficacy. The mitochondrial targeting ability of the MTSs was determined on the basis of the ratio of MTS-green fluorescent protein (GFP) expressed in the cytosol to that expressed in the mitochondria (Figure 1). The plasmid DNA (pDNA), *P35S-MTS-GFP-Tnos*, was designed to express MTS-GFP in the cytosol (Figure S1). MTS-GFP was delivered to mitochondria in a manner dependent on the function of the MTS. To introduce the pDNA to the nucleus with particle bombardment, we prepared gold nanoparticle/pDNA complexes by mixing gold nanoparticles and pDNA. The complexes were introduced into the leaves of the MTS-Red fluorescent protein (RFP) ox-*A. thaliana*[30] via a particle gun. The mitochondria of MTS-RFP ox-*A. thaliana* were fluorescently labeled with RFP. After incubation for 18 h, the leaves were observed via confocal laser scanning microscopy (CLSM). *P35S-eGFP-Tnos* was used as the negative control. Without an MTS, untagged GFP localizes to the cytosol. GFP fluorescence was observed throughout the cytoplasm under the control conditions (Figure 2A). If the MTS tag at the N-terminus of GFP has a high mitochondrial targeting function, the GFP fluorescence will colocalize with the mitochondria. For Cytcox12 (Figure 2B), GFP was observed in the cytoplasm and mitochondria. In contrast, GFP was localized in the mitochondria of the Cytcox25, SD3, and HSP60 groups (Figure 2C–E). These findings indicate that Cytcox25, SD3, and HSP60 had MTSs that were better than did Cytcox12. Next, the colocalization ratio of GFP expression and mitochondria was quantified. The colocalization ratio was defined as the ratio of the number of

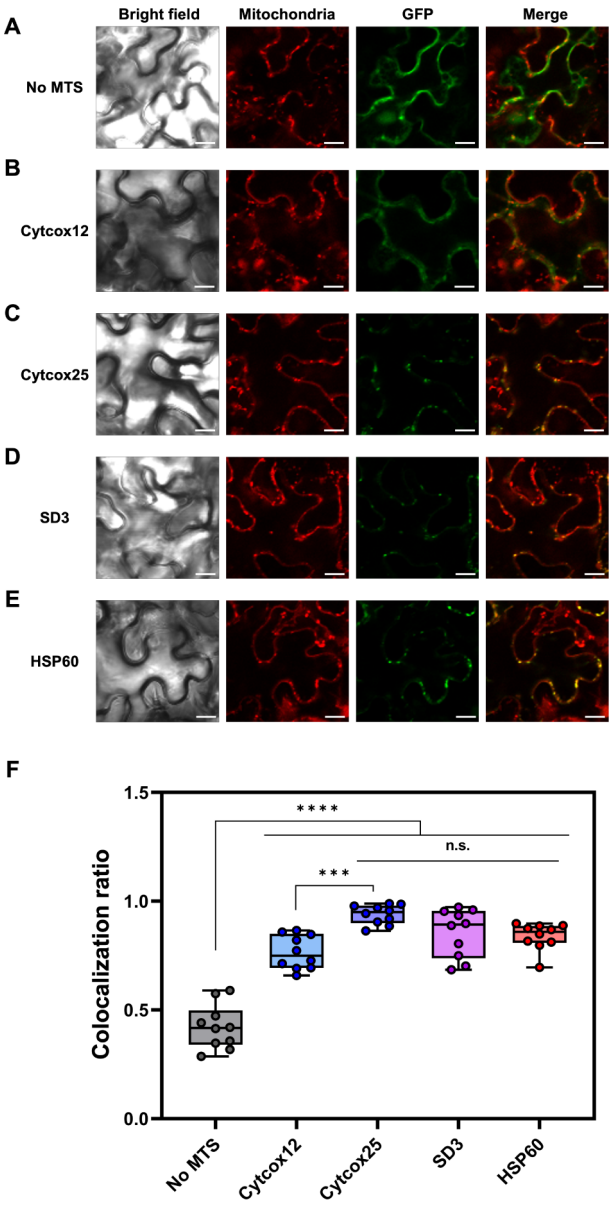

Figure 2. Colocalization analysis of some presequences. (A–E) Representative CLSM images of (A) no MTS, (B) Cytcox12, (C) Cytcox25, (D) SD3, and (E) HSP60. Scale bars: 10 μm. (F) The colocalization ratio of some presequences. Statistical significance was set at $p > 0.05$ (n.s.), $p < 0.001$ (***), and $p < 0.0001$ (****) on the basis of Tukey's multiple comparison tests ($n = 10$).

GFP pixels in mitochondria to the number of all GFP pixels. Here, we used the colocalization ratio as an index of the mitochondrial targeting function of each MTS. The obtained CLSM images were analyzed with ImageJ to calculate the

https://doi.org/10.1021/acschembio.4c00625
ACS Chem. Biol. 2024, 19, 2515–2524

A

```
A. thaliana      MYRFASNLASKARIAQN---ARQVSSRMSWSRNYAA
B. napus         MYRLISSIASKARVARNC--TSQIGSRLSSTRNYAA
N. tabacum       MYRFAASLASKARVARTS--TQQIGGRLNWSRNYAA
S. tuberosum     MYRFAANLASKASVARTS--SQKIGGRLNWSRNYAA
S. lycopersicum  MYRFAANLASKARVARIS--SQQIGGRFNWSRNYAA
O. sativa        MYRAAASLASKARQAGSS--ARQVGSRLALSRNYAA
Z. mays          MYRAAASLASKARQAGSSSAARQVGSRLAWSRNYAA
                 ***  :.:****  *     : ::..*:  :*****
```

B

	A. thaliana	B. napus	N. tabacum	S. lycopersicum	S. tuberosum	O. sativa	Z. mays
A. thaliana		60.61	63.64	60.61	66.67	69.70	72.73
B. napus	60.61		67.65	55.88	58.82	58.82	58.82
N. tabacum	63.64	67.65		88.24	88.24	70.59	73.53
S. lycopersicum	60.61	55.88	88.24		88.24	61.76	64.71
S. tuberosum	66.67	58.82	88.24	88.24		64.71	67.65
O. sativa	69.70	58.82	70.59	61.76	64.71		97.08
Z. mays	72.73	58.82	73.53	64.71	67.65	97.06	

Percent identity matrix (%)
- 90.00~99.99
- 80.00~89.99
- 70.00~79.99
- 60.00~69.99
- ~59.99

Figure 3. Multiple sequence alignment of HSP60 presequences in various model plants via T-coffee. *A. thaliana*, *B. napus*, *N. tabacum*, *S. lycopersicum*, *S. tuberosum*, *O. sativa*, and *Z. mays* are abbreviations for *Arabidopsis thaliana*, *Brassica napus*, *Nicotiana tabacum*, *Solanum lycopersicum*, *Solanum tuberosum*, *Oryza sativa*, and *Zea mays*, respectively. (A) Alignment result. Cyan colors with an asterisk (*) indicate positions with a single amino acid residue. Yellow colors with a colon (:) indicate conservation between groups with strongly similar properties. Magenta colors with a dot indicate the conservation between groups with weakly similar properties. (B) PIM between each alignment. The PIM indicates the percentage of conservation between each alignment.

colocalization ratio (Figure 2F). The colocalization ratio of Cytcox12 was lower than that of Cytcox25. This finding shows that the mitochondrial targeting function of Cytcox was partially lost by shortening the sequence to 12 residues. Cytcox was shortened to focus on the generally representative amino acids in MTSs, such as lysine, arginine, serine, and threonine.[25] However, it is becoming clear that the secondary structure is also important for the ability of MTSs to target mitochondria. The presequences of mitochondrial protein precursors form the helical structure, and the cationic and hydrophobic regions in the structure are recognized by the TOM.[14] The secondary structure of the MTS needs to be considered when the MTS is shortened. The plant-derived MTSs SD3 and HSP60 presented high mitochondrial targeting efficacy, similar to that of Cytcox25. The presequences of SD3 and HSP60 are promising plant-derived MTSs.

Multiple Sequence Alignment of MTSs Among Several Model Plants. The presequence of HSP60 derived from *N. tabacum* showed high mitochondrial targeting ability even in *A. thaliana*. To investigate the versatility of HSP60 in various plants, we performed multiple sequence alignment of HSP60 presequences in several model plants. We chose *A. thaliana*, *Brassica napus*, *N. tabacum*, *Oryza sativa*, *Solanum lycopersicum*, *Solanum tuberosum*, and *Zea mays* as model plants. The cleavage site of each HSP60 precursor was predicted with TargetP-2.0, and then the N-terminal presequence was used for multiple sequence alignment. The alignment was performed via T-coffee.[31,32] The HSP60 presequences showed high similarity in this alignment (Figures 3A and S2). In Figure 3B, the percent identity matrix (PIM) between each aligned sequence is shown. The PIM is the score determined for each pair of aligned sequences and shows the similarity between the two sequences. The PIM of the HSP60 presequences was greater than 50 for all pairs. In particular, the PIM of *N. tabacum* was high overall. In contrast, multiple sequence alignment was also performed for the SD3 presequence, which showed a high mitochondrial-targeting ability, as did the HSP60 presequence. However, the SD3 presequence was barely conserved among the selected model plants (Figure S3). These results indicate that the HSP60 presequence of *N. tabacum* is a powerful MTS in many plant species.

Design of the Shortened HSP60 MTS by Secondary Structure Prediction. As shown above, the sequence of HSP60 derived from *N. tabacum* has the potential to be an effective MTS in many plant species. However, using this original sequence for delivery to plant mitochondria is difficult because peptides consisting of 34 amino acid residues are too long to be synthesized via common solid-phase peptide synthesis. Generally, the synthesis of long peptides is impractical due to their low yield. A shortened presequence is usually used for modifying gene carriers. When the presequence is shortened, it is important to maintain the efficacy of mitochondrial targeting. The helical structure of MTSs is crucial for recognition by TOM.[33] Next, we designed several candidate sequences for HSP60 presequence shortening on the basis of a secondary structure. We utilized AlphaFold 3[34] to predict the secondary structures of the candidate sequences. The predicted secondary structures of some shortened HSP60 presequences are shown in Figure 4. The sequences were shortened from the HSP60 presequence, leaving the N-terminus to maintain their mitochondrial targeting function.[16,17] The sequences from the N-terminus to the alanine of the ninth residue, to the serine of the 10th residue, to the lysine of the 11th residue, to the alanine of the 15th residue, and to the glutamine of the 20th residue were called N9, N10, N11, N15, and N20, respectively. N34 is the full length of the HSP60 presequence. The amino acid sequences are shown in Table 2. In Figure 4, the predicted structures are ranked in order of their ranking score, indicating the reliability of the prediction. The ranking score was calculated on AlphaFold 3 on the basis of the predicted local distance difference test (pLDDT), the predicted alignment error (pAE), and the predicted distance error (pDE). In AlphaFold 3, N11 and longer sequences were predicted to form helical structures as well as the full-length HSP60 presequence (Figure 4C−F), but the helical structure was destabilized in N9 (Figure 4A). Among the predicted

https://doi.org/10.1021/acschembio.4c00625
ACS Chem. Biol. 2024, 19, 2515−2524

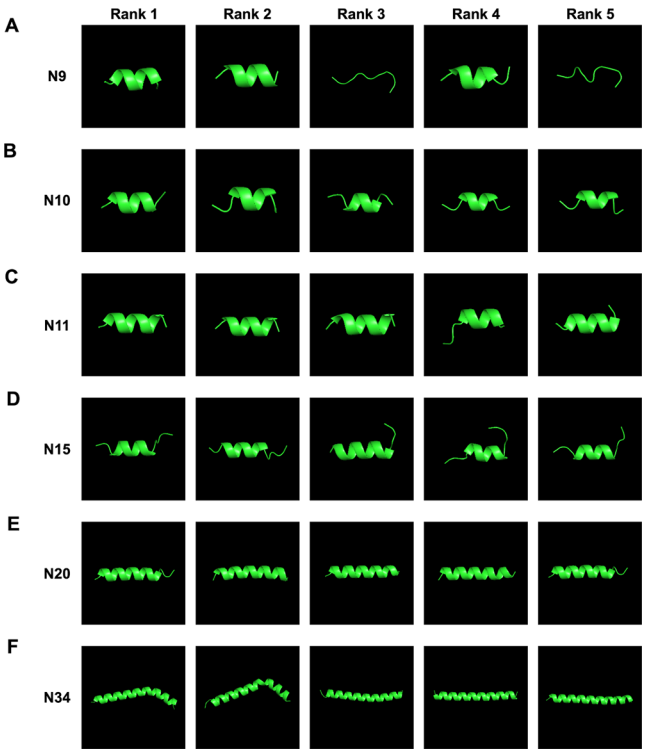

Figure 4. Predicted secondary structures of (A) N9, (B) N10, (C) N11, (D) N15, (E) N20, and (F) N34. These secondary structures were predicted using AlphaFold 3. The predicted structures were ranked in order of their ranking score. The ranking score indicates the reliability of the prediction and is calculated on AlphaFold 3 from pLDDT, pAE, and pDE. Rank 1 is the most reliable structure in the sequence.

structures of N10, the helical structure destabilized for most of the sequences (Figure 4B). The secondary structures of Cytcox12 and Cytcox25 were also predicted using AlphaFold 3. The helical structure was dominant in the prediction of Cytcox12 and 25, but the N-termini of Cytcox12 and 25 formed a random structure (Figure S4). In view of this secondary structure prediction, we chose these sequences as candidates for the shortened HSP60 MTS (Table 2). Additionally, to confirm the reliability of the prediction, circular dichroism (CD) was used for each candidate sequence (Figure S5). The shortened HSP60 presequences and Cytcox12 were synthesized via solid-phase peptide synthesis (Figure S6). The peptides were dissolved in 1% sodium dodecyl sulfate (SDS) solution for CD measurements to estimate the secondary structure of the MTSs near the mitochondrial membrane.[35] The spectrum of Cytcox12 exhibited a positive peak at 197 nm and a negative peak at 218 nm, which are typical of an β sheet structure. The CD spectrum of N20 was also typical of a β sheet structure. These results for Cytcox12 and N20 were not consistent with the AlphaFold 3 predictions. Figures 4E and S4A show the predicted structures of the single peptide molecules, and therefore Cytcox12 and N20 would form intermolecular β sheet structures in the CD measurements. With respect to the other HSP60 presequence, the spectrum of N34 exhibited a positive peak at 192 nm and negative peaks at 207 and 222 nm, which are typical of a helical structure. The peaks suggesting a helical structure could also be observed in the spectra of N11 and N15. However, the spectra of N9 and N10 showed a negative peak at 198 nm, which is typical of a random structure. These CD spectra indicate that the predicted secondary structures of the shortened HSP60 presequences are mostly identical to the actual conformation in the environment that mimics the vicinity of the mitochondria.

Mitochondrial Targeting Efficacy of the Short HSP60 MTS. The mitochondrial targeting efficiency of the chosen candidate sequences was evaluated by the colocalization of mitochondria and MTS-GFP expressed in the cytosol. The *P35S-MTS-GFP-Tnos* for each shortened candidate sequence was introduced into the nucleus of an MTS-RFP ox-*A. thaliana* leaf with a particle gun, and the localization of the expressed MTS-GFP was analyzed via CLSM observation and image analysis. The obtained CLSM images are shown in Figure 5A-E. When the sequence length was less than 11 amino acid residues, GFP expression was observed throughout the cytoplasm (Figure 5A−C). For N15 and N20, GFP was localized in the mitochondria (Figure 5D,E). The localization of GFP tagged with N15 or N20 was similar to that of full-length HSP60 MTS (Figure 3E). Even though the secondary structure of N20 was estimated as β sheets on the basis of the CD spectrum (Figure S5), N20 exhibited high mitochondrial targeting function in this reporter protein sorting analysis. This is probably because the N20 tagged at the N-terminus of GFP is less likely to interact with the other N20 sequence. The obtained CLSM images were analyzed with ImageJ to quantify the mitochondrial targeting efficacy of each sequence (Figure 5F). The mitochondrial targeting function was maintained in N15 and the longer sequences. In contrast, the colocalization ratio significantly decreased with N11, although the N11 sequence was predicted to form a helical structure by AlphaFold3. The helical structure of N11 might be more unstable in plant cells than that predicted by AlphaFold 3. For N9 and N10, GFP fluorescence was mainly observed in the cytosol, indicating the low mitochondrial targeting ability of N9 and N10 (Figure 5A,B). The low efficacy of N9 and N10

Table 2. New MTS Candidates Derived from HSP60 Presequences[a]

MTS	Sequence	Prediction score
N9	MYRFAASLA	N/A
N10	MYRFAASLAS	0.3652
N11	MYRFAASLASK	0.4667
N15	MYRFAASLASKARVA	0.5259
N20	MYRFAASLASKARVARTSTQ	0.6286
N34 (Full length)	MYRFAASLASKARVARTSTQQIGGRLNWSRNYAA	0.6847

[a]The sequences from the N-terminus to the alanine of the 9th residue, to the serine of the 10th residue, to the lysine of the 11th residue, to the alanine of the 15th residue, and the glutamine of the 20th residue were called N9, N10, N11, N15, and N20, respectively. N34 is the full length of the HSP60 presequence. The predicted probability for the mitochondrial targeting peptide is displayed as a prediction score

https://doi.org/10.1021/acschembio.4c00625
ACS Chem. Biol. 2024, 19, 2515−2524

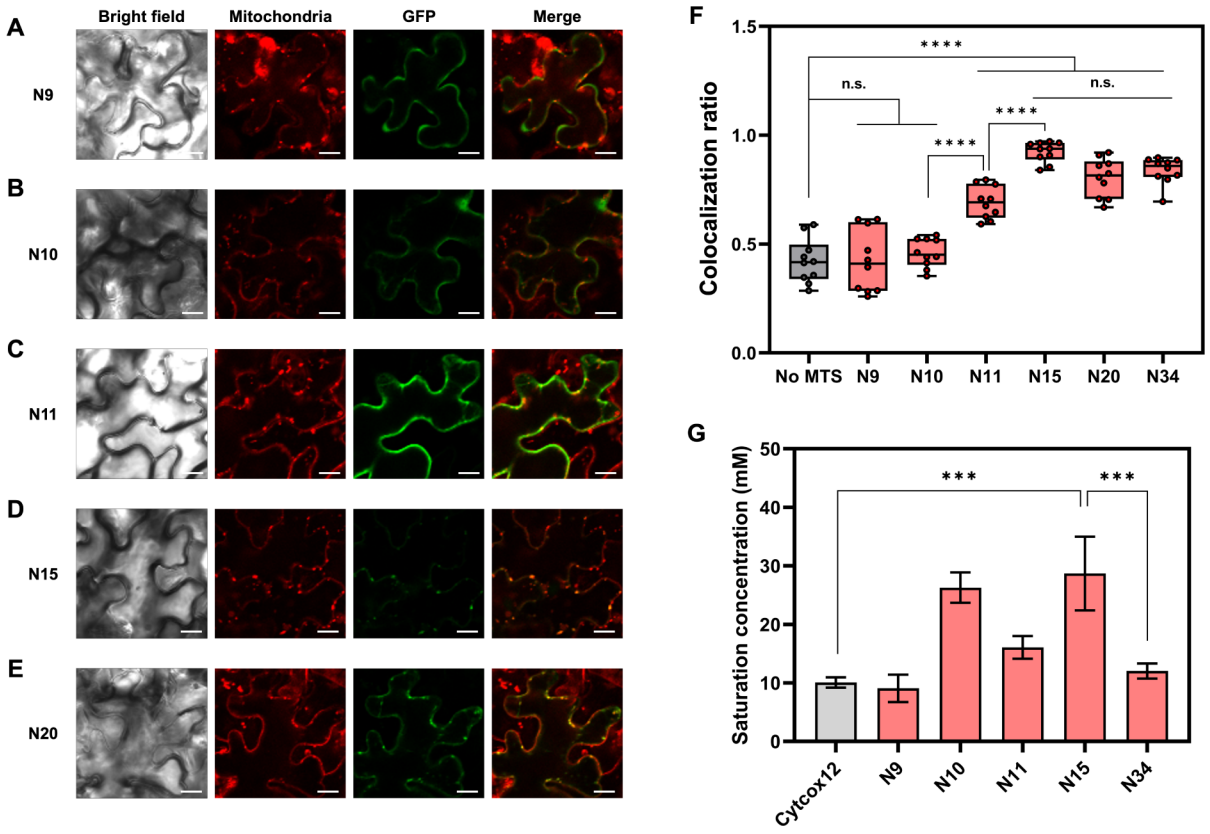

Figure 5. (A–F) Colocalization analysis. (A–E) Representative CLSM images of (A) N9, (B) N10, (C) N11, (D) N15, and (E) N20. The white arrows in (D) and (E) indicate the mitochondria overlapping with GFP. Scale bars: 10 μm. (F) The colocalization ratio of each HSP60 MTS candidate. Statistical significance was set at $p > 0.05$ (n.s.) and $p < 0.0001$ (****) on the basis of tukey's multiple comparisons tests ($n = 10$). (G) The saturation concentration of each MTS. The statistical significance was set at $p < 0.001$ (***) on the basis of tukey's multiple comparison tests ($n = 3$). The vertical bars indicate standard deviations.

may be due to the instability of their helical structures (Figures 4A,B and S5). The trend of the mitochondrial targeting efficacy was slightly different from that of the secondary structure prediction of the shortened sequence, but the secondary structure prediction seems to be helpful for designing short and effective MTSs. The results revealed that N15 and longer sequences are effective MTSs in *A. thaliana*.

Solubility of the Shortened HSP60 Presequences. N15 had a greater effect on mitochondrial targeting than did Cytcox12. To determine whether N15 could be used for gene delivery in an aqueous system, we assessed the solubility of N15. The saturation concentrations of the shortened HSP60 presequences were evaluated to compare their solubilities in water (Figure 5G). The saturation concentrations of N15 and N34 were 28.69 ± 6.31 and 12.04 ± 1.29 mM, respectively, suggesting that the solubility of the presequence of HSP60 is improved by sequence shortening. In contrast, the saturation concentration of Cytcox12 was 9.07 ± 2.33 mM. Also, the saturation concentration of N20 could not be evaluated because the N20 solution gelatinized during the preparation of the saturated N20 solution. The results of this solubility test indicate that N15 has an advantage in the preparation of an MTS-modified carrier. The highly soluble MTS increased the stability of the MTS-modified carrier, and the modification rate of the MTS can be increased to promote the delivery efficacy to plant mitochondria. N15 would be a useful MTS for delivery to plant mitochondria.

Validity of N15 Among Different Model Plant Species. As mentioned above, N15 is a valuable MTS in terms of its mitochondrial targeting ability and solubility. Interestingly, the N15 sequence of HSP60 is conserved among the various model plants. This phenomenon indicates that N15 may be an effective MTS in a wide variety of plant species. To investigate the validity of N15 in different plant species, we analyzed the localization of fluorescently labeled N15 in four model plant species. Rhodamine-labeled N15 and KAibA, which is a cell-penetrating peptide, were synthesized. The rhodamine-labeled peptides were called N15-Rho [MYRFAAS-LASKARVAK (Rho), Rho: rhodamine] and KAibA-Rho [KXAKXAKXAK(Rho), *X*: 2-aminoisobutyric acid], respectively. Rhodamine was modified with the side chain amine of the C-terminal lysine. This experiment used wild-type *A. thaliana*, *N. tabacum*, *S. lycopersicum*, and *O. sativa* as model plants. *A. thaliana*, *N. tabacum*, and *S. lycopersicum* are dicots, and *O. sativa* is a monocot. Each rhodamine-labeled peptide solution was infiltrated into the leaf of each model plant, and the leaf was observed via CLSM (Figure 6). KAibA did not localize to mitochondria in any of the model plants (Figure 6B,D,F,H). In contrast, N15 colocalized with mitochondria in dicots (Figure 6A,C,E). Furthermore, the colocalization of N15 and mitochondria was confirmed in *O. sativa* (Figure 6G). This result indicates that N15 from *N. tabacum* has an effective mitochondrial targeting function not only in dicotyledonous plants but also in monocotyledonous plants. N15 is considered to be an effective and versatile MTS in a variety of plants.

https://doi.org/10.1021/acschembio.4c00625
ACS Chem. Biol. 2024, 19, 2515–2524

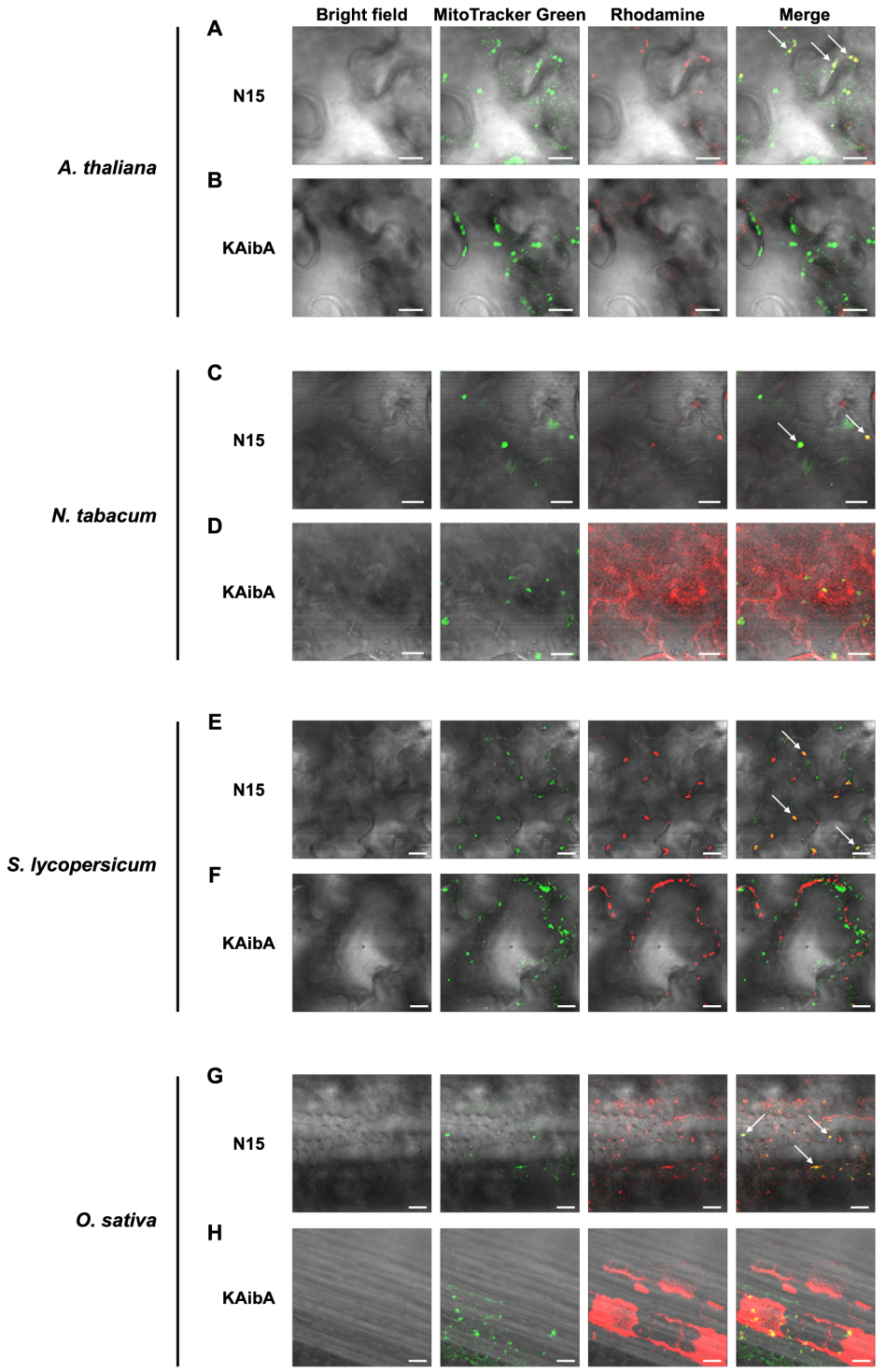

Figure 6. Validity of N15 in different model plants. KAibA without a mitochondrial targeting function was used as the negative control. The peptides were labeled with rhodamine. As model plants, (A,B) *A. thaliana*, (C,D) *N. tabacum*, (E,F) *S. lycopersicum*, and (G,H) *O. sativa* were used. The CLSM images of N15 and KAibA are shown in (A,C,E,G) and (B,D,F,H), respectively. The white arrows indicate that the mitochondria colocalized with the rhodamine-labeled peptide. Scale bars = 10 μm.

However, the cellular uptake of the rhodamine-labeled N15 may not have been sufficient in *O. sativa*. In a previous report, no cell-penetrating peptide was shown to be internalized by *O. sativa*.[36] Monocotyledonous plants, such as *O. sativa*, generally accumulate large amounts of silicon, and their cells are surrounded by a silica layer.[37] The silica barrier is thought to protect cells from exogenous substances. To introduce bioactive materials into the mitochondria of monocots, we need a strategy to overcome the silica layer. The results of this study indicate that the cellular uptake of N15 may be low, but N15 has a mitochondria-targeting function, even in rice cells. Furthermore, we investigated the cytotoxicity and its effect on mitochondrial membranes. Cytotoxicity was evaluated on the basis of the Evans Blue assay (Figure S8A,B). Evans Blue fluorescence is confirmed in the dead cells, because Evans Blue can penetrate only into dead cells. These results showed low

https://doi.org/10.1021/acschembio.4c00625
ACS Chem. Biol. 2024, 19, 2515−2524

cytotoxicity of N15 in root cells and epidermal cells of *A. thaliana*. Mitochondrial membrane potential was evaluated using tetramethyl rhodamine ethyl ester (TMRM) (Figure S9). The mitochondria with a normal membrane potential are labeled with TMRM, but the TMRM fluorescence in mitochondria weakens or disappears when the mitochondrial membrane potential declines. At 10 μM N15, mitochondria were labeled with mitochondria, indicating that 10 μM N15 did not affect the mitochondrial membrane potential. In contrast, TMRM was not localized into mitochondria at 100 μM N15, indicating the effect on the mitochondrial membrane potential at a high concentration of N15. However, a 10 μM solution of N15 was used for the validity test for N15 in this work. In addition, MTS concentrations lower than 10 μM have been used for the delivery of bioactive substances to plant mitochondria.[23] In short, N15 would not affect the mitochondrial membrane potential at the delivery of bioactive substances.

CONCLUSIONS

Presequences are helpful tools for delivery systems to mitochondria, but sequence shortening of presequences is often required when chemically synthesized presequences are used as delivery carriers. In this study, we presented a useful approach for chemically designing signal sequences on the basis of biological information. Combining this *in silico* approach with the experimental method, we developed an effective MTS, N15. N15 is the 15-terminal 15 residue of HSP60 derived from *N. tabacum*. N15 was designed on the basis of the secondary structure prediction by AlphaFold 3 and was conserved among various model plants according to multiple sequence alignment. N15 showed high mitochondrial targeting efficacy and solubility. Additionally, according to the alignment results, the conservation of N15 among different model plants indicated that N15 is a valid MTS in various plant species. The validity of N15 was experimentally confirmed in *A. thaliana*, *N. tabacum*, *S. lycopersicum*, and *O. sativa*. N15 is expected to be an effective MTS in many plant species. Additionally, the MTS design approach, which is based on biological information, was considered reasonable in this work. Biological information helps in the design of valuable ligands with characteristic structures and meaningful sequences. We can develop the desired signal molecule following this *in silico* approach without substantial screening. In the future, more biological information will be accumulated in databases and more reasonable ligand designs will be possible.

EXPERIMENTAL SECTION

Plasmid DNA. *P35S-eGFP-Tnos*, which harbors a cauliflower mosaic virus 35S promoter, eGFP, and a nopaline synthase terminator for nuclear expression with eGFP, was used as a vector to prepare *P35S-MTS-eGFP-Tnos* (Figure S1). MTSs amplified by PCR were inserted between the *Sal*I and NcoI sites of *P35S-eGFP-Tnos*. All sequences of primers used in this work are shown in Table S1.

Plant Material and Growth Condition. Transgenic *A. thaliana* (Columbia) plants expressing RFP fused to the F1-ATPase delta-prime subunit (MTS-RFP ox) were kindly provided by Dr. Shin-ichi Arimura (The University of Tokyo, Japan).[30] Transgenic *A. thaliana* was used for the particle bombardment experiments. The sterilized seeds of the transgenic *A. thaliana* were cultivated for 2 months in a 2:1 mixture of soil and vermiculite at 22 °C under 16/8 h light/dark periods. Wild types of *A. thaliana*, *N. tabacum*, *S. lycopersicum*, and *O. sativa* were used for the validity assay of N15. *A. thaliana* was grown under daylength conditions of 16/8 h light/dark periods at 22 °C. For *N. tabacum* and *S. lycopersicum*, seeds were sown and cultivated in soil supplemented with vermiculite at a ratio of 2:1 and incubated at 28 °C with 14/10 h light/dark periods. For *O. sativa*, peeled seeds were sterilized with 70% ethanol for 1 min followed by 0.5% sodium hypochlorite for 20 min with rotation and then washed with sterilized water. The sterilized rice seeds were cultivated on MS medium and incubated at 30 °C in the dark.

Preparation of the pDNA/AuNP Complex. One milliliter of ice-cold 70% ethanol was added to 20 mg of 0.6 μm gold nanoparticles (Bio-Rad, CA, U.S.A.). The mixture was vortexed vigorously for 5 min and then incubated for 10 min at RT. After centrifugation at 600 × *g* for 1 min, the sap was removed. One milliliter of ice water was added to the precipitate, and the mixture was vortexed. After the mixture was left at RT for 5 min, it was centrifuged and the sap was removed as described above. One milliliter of ice water was added again, and the mixture was vortexed. The mixture was incubated at RT for 5 min. After incubation, the mixture was centrifuged at 1700 × g for 15 s, and then the sap was removed completely. Five hundred microliters of distilled water was added to the precipitate, after which the mixture was sonicated for 1 min. For coating of the gold nanoparticles with pDNA, 20 μL of the gold nanoparticle suspension, 4 μg of pDNA, 20 μL of 2.5 M calcium chloride, and 8 μL of 0.1 M spermidine were added to a 1.5 mL tube in this order, after which the mixture was vortexed for at least 3 min. The mixture was subsequently incubated on ice for more than 5 min. The mixture was subsequently centrifuged at 2000 × *g* for 5 s, after which the sap was removed. The centrifuged gold nanoparticles were washed with 70% ethanol and then with 100% ethanol, and the gold nanoparticles were finally resuspended in 30 μL of 100% ethanol.

Particle Bombardment. The bombardment experiments were performed according to a previous report.[38] Fifteen microliters of the prepared pDNA/AuNP complex mixture was dropped on a plastic disk. The solvent was dried under an atmospheric pressure. The four rosette leaves of MTS-RFP ox-*A. thaliana* were set on 1/2 MS agar medium with the backside of the leaves up. The leaves on the agar medium were set in the chamber of the particle gun (PDS-1000/He System, Bio-Rad). Particle bombardment was performed twice for each plate at 1100 psi, and the inside of the particle gun was depressurized at −28 mmHg during bombardment. After bombardment, the leaves were incubated for 18 h under dark growth conditions.

CLSM. After 18 h of incubation, the leaves introduced with the pDNA/AuNP complexes were cut into quarters. The leaves were observed via CLSM (LSM700, Carl Zeiss, Oberkochen, Germany) with a 20× objective at 488 nm for GFP.

Image Analysis. The obtained CLSM images were analyzed via ImageJ. Each GFP-expressing cell was cut from the image along its outline. GFP and RFP are colored green and red, respectively. The red and green colors in the image were split into different channels. The GFP and RFP channels were analyzed via the JACoP plugin to obtain the colocalization ratio.[39] The colocalization ratio was defined as the ratio of the number of GFP pixels overlapping RFP pixels to the number of all of the GFP pixels.

Secondary Structure Prediction. The secondary structure prediction was performed on the AlphaFold server powered by AlphaFold 3.[34] The predicted structures of each sequence were ranked from 1 to 5 in the order of the ranking score. The ranking score was calculated on AlphaFold 3 from pLDDT, pAE, and pDE.

Peptide Synthesis. All peptides used in this work were synthesized via solid-phase peptide synthesis using 9-fluorenyl methoxycarbonyl amino acids. These syntheses were performed with an automatic synthesizer (Liberty Blue 2.0, CEM, NC, U.S.A.). The reagents used for peptide synthesis were purchased from FUJIFILM Wako Pure Chemical (Osaka, Japan), Tokyo Chemical Industry (Tokyo, Japan), and Watanabe Chemical Industries (Hiroshima, Japan). The N-termini of all synthesized peptides were unprotected, and the C-termini of those were amides. After synthesis, the peptides were purified by reverse-phase high-performance liquid chromatography (RP-HPLC). The HPLC system consisted of a SIL-40C autosampler, an LC-40D gradient pomp, a DGU-405 degassing

https://doi.org/10.1021/acschembio.4c00625
ACS Chem. Biol. 2024, 19, 2515−2524

unit, a FRC-10A fraction collector, and an SPD-M40 photodiode array detector (Shimadzu Corporation, Kyoto, Japan). A $5C_{18}$-MS-II column (NACALAI TESQUE, INC., Kyoto, Japan) was used for peptide purification. The mobile phase comprised acetonitrile (A) and water (B) containing 0.1% trifluoroacetic acid. The acetonitrile gradient conditions were 18−20%, 20−30%, 17−18%, 20−21%, 18−21%, 22−25%, and 25−30% for N9, N10, N11, N15, N20, N34, and Cytcox purification, respectively. The analysis time was 30 min. The purity of the purified peptides was analyzed with the same HPLC system as described above. The acetonitrile gradient condition was 5−90% (10 min). The molecular weights of the obtained peptides were analyzed with ultrafleXtreme (Bruker Corporation, MA, U.S.A.).

CD Measurement. Each peptide powder was dissolved in a 1% SDS aqueous mixture. The peptide concentration was fixed at 150 μM. CD spectra were recorded at 25 °C on a JASCO J-1500 CD spectrometer (JASCO, Tokyo, Japan).

Multiple Sequence Alignment. Multiple sequence alignment was performed via the EMBL-EBI web resource.[40] This work used T-Coffee for the multiple sequence alignment programs.[31,32]

Solubility Test. The peptide powder was added to 30 μL of water to prepare the saturated peptide solution. The saturated solution was vortexed for 10 s, after which the mixture was centrifuged for 5 min at 15000 rpm. The sap was lyophilized, and the obtained peptide powder was subsequently weighed to calculate the saturated concentration.

Validity of N15 in Different Model Plants. All leaves used in this experiment were degassed before peptide treatment. Two hundred microliters of 10 μM rhodamine-labeled peptide solution dissolved in 1% dimethyl sulfoxide (FUJIFILM Wako Pure Chemical) was infiltrated into each leaf of *A. thaliana*, *N. tabacum*, or *S. lycopersicum* with a 1 mL syringe. In the case of *O. sativa*, the leaf was placed in a 10 μM rhodamine-labeled peptide solution. Afterward, the leaves of *O. sativa* were placed in a reducing environment (−0.08 MPa) for one min and then in a pressurized environment (0.08 MPa) for 1 min. Two hours after infiltration, each leaf was stained with 100 nM MitoTracker Green FM (Thermo Fisher, MA, U.S.A.). After another hour, each leaf was observed via CLSM.

Cytotoxicity Assay. Cytotoxicity of N15 was evaluated by using Evans Blue. Evans Blue was purchased from FUJIFILM Wako Pure Chemical. The seedlings of *A. thaliana* were used as model plants in this experiment. To prepare 100% dead samples, the seedlings were dipped into 98 °C water for 30 min. To prepare 0% dead samples, the seedlings were dipped into 25 °C water for 30 min. To treat the seedling with N15 solution, a seedling was dipped into 10 or 100 μM N15 aqueous solution for 30 min at 25 °C. After treatment with peptide or water, the seedlings were stained with 150 mg/L Evans Blue aqueous solution for 30 min at 25 °C. The stained seedlings were washed with water, and then, the seedlings were observed with CLSM.

Mitochondrial Membrane Analysis. Mitochondrial membrane potential was evaluated by TMRM. TMRM was purchased from Thermo Fisher. The seedlings of *A. thaliana* were dipped into water, or 10 or 100 μM N15 aqueous solution for 30 min. After the seedlings were washed with water, the seedlings were stained with 100 nM TMRM for 30 min. After that, the seedlings were observed with CLSM.

Statistical Analysis. The statistical significance of differences in the colocalization tests and the solubility tests were analyzed by tukey's multiple comparisons tests. The statistical significance was set at $p > 0.05$ (n.s.), $p < 0.05$ (*), $p < 0.01$ (**), $p < 0.001$ (***), and $p < 0.0001$ (****).

■ ASSOCIATED CONTENT

Supporting Information

The following file is available free of charge:The Supporting Information is available free of charge at https://pubs.acs.org/doi/10.1021/acschembio.4c00625.

Schematic illustration of subcloning; multiple sequence alignment of HSP60; multiple sequence alignment of SD3; secondary structure prediction of Cytcox12 and Cytcox25; CD spectra of the shortened HSP60 presequences; characterization of the synthesized presequences; characterization of the rhodamine-labeled peptides; and sequences of primers used for subcloning in this work (PDF)

■ AUTHOR INFORMATION

Corresponding Author

Keiji Numata − *Department of Material Chemistry, Graduate School of Engineering, Kyoto University, Kyoto, Nishikyo-ku 615-8510, Japan; Biomacromolecules Research Team, RIKEN Center for Sustainable Resource Science, Saitama, Wako 351-0198, Japan;* orcid.org/0000-0003-2199-7420; Email: keiji.numata@riken.jp

Authors

Naoya Abe − *Department of Material Chemistry, Graduate School of Engineering, Kyoto University, Kyoto, Nishikyo-ku 615-8510, Japan*

Masaki Odahara − *Biomacromolecules Research Team, RIKEN Center for Sustainable Resource Science, Saitama, Wako 351-0198, Japan*

Shamitha Rao Morey − *Department of Material Chemistry, Graduate School of Engineering, Kyoto University, Kyoto, Nishikyo-ku 615-8510, Japan;* orcid.org/0000-0002-0971-0653

Complete contact information is available at: https://pubs.acs.org/10.1021/acschembio.4c00625

Author Contributions

M.O., S.R.M., and K.N. conceived and designed the research. N.A., M.O., and K.N. wrote the manuscript. N.A. and M.O. performed all the experiments. N.A. analyzed all the data.

Notes

The authors declare no competing financial interest.

■ ACKNOWLEDGMENTS

Transgenic *A. thaliana*(Columbia) plants containing fluorescent mitochondria expressing red fluorescent protein fused to the F1-ATPase delta-prime subunit (Mt-RFP) were kindly provided by Dr. Shin-ichi Arimura (The University of Tokyo, Japan). This work was supported by the JST, the establishment of university fellowships towards the creation of science technology innovation (Grant Number JPMJFS2123), the Grant-in-Aid for Transformative Research Areas (A) (Grant Number 24H02272), the JST-COI-NEXT (Grant Number JPMJPF2114), and the MEXT Data Creation and Utilization-type MaTerial R&D project.

■ REFERENCES

(1) Tilman, D.; Balzer, C.; Hill, J.; Befort, B. L. Global food demand and the sustainable intensification of agriculture. *Proc. Natl. Acad. Sci. U. S. A.* **2011**, *108*, 20260−20264.

(2) Foley, J. A.; Defries, R.; Asner, G. P.; Barford, C.; Bonan, G.; Carpenter, S. R.; Chapin, F. S.; Coe, M. T.; Daily, G. C.; Gibbs, H. K. Global consequences of land use. *Science* **2005**, *309*, 570−574.

(3) Godfray, H. C.; Beddington, J. R.; Crute, I. R.; Haddad, L.; Lawrence, D.; Muir, J. F.; Pretty, J.; Robinson, S.; Thomas, S. M.; Toulmin, C. Food security: The challenge of feeding 9 billion people. *Science* **2010**, *327*, 812−818.

(4) Tilman, D.; Fargione, J.; Wolff, B.; D'Antonio, C.; Dobson, A.; Howarth, R.; Schindler, D.; Schlesinger, W. H.; Simberloff, D.;

Swackhamer, D. Forecasting agriculturally driven global environmental change. *Science* **2001**, *292*, 281−284.
(5) Grassini, P.; Eskridge, K. M.; Cassman, K. G. Distinguishing between yield advances and yield plateaus in historical crop production trends. *Nat. Commun.* **2013**, *4*, 2918.
(6) Bohnert, H. J.; Gong, Q.; Li, P.; Ma, S. Unraveling abiotic stress tolerance mechanisms–getting genomics going. *Curr. Opin. Plant Biol.* **2006**, *9*, 180−188.
(7) Apse, M. P.; Blumwald, E. Engineering salt tolerance in plants. *Curr. Opin. Biotechnol.* **2002**, *13*, 146−150.
(8) Wang, W.; Vinocur, B.; Altman, A. Plant responses to drought, salinity and extreme temperatures: Towards genetic engineering for stress tolerance. *Planta* **2003**, *218*, 1−14.
(9) Spinelli, J. B.; Haigis, M. C. The multifaceted contributions of mitochondria to cellular metabolism. *Nat. Cell Biol.* **2018**, *20*, 745−754.
(10) Hanson, M. R.; Bentolila, S. Interactions of mitochondrial and nuclear genes that affect male gametophyte development. *Plant Cell* **2004**, *16* (Suppl), S154−169.
(11) Wang, Y. H.; Ying, Y.; Chen, J.; Wang, X. C. Transgenic overexpressing Mn-SOD enhanced salt-tolerance. *Plant Sci.* **2004**, *167*, 671−677.
(12) Hay, R.; Bohni, P.; Gasser, S. How Mitochondria Import Proteins. *Biochim. Biophys. Acta.* **1984**, *779*, 65−87.
(13) Pfanner, N.; Douglas, M. G.; Endo, T.; Hoogenraad, N. J.; Jensen, R. E.; Meijer, M.; Neupert, W.; Schatz, G.; Schmitz, U. K.; Shore, G. C. Uniform nomenclature for the protein transport machinery of the mitochondrial membranes. *Trends Biochem. Sci.* **1996**, *21*, 51−52.
(14) Pfanner, N. Mitochondrial import: Crossing the aqueous intermembrane space. *Curr. Biol.* **1998**, *8*, R262−265.
(15) Sjöling, S.; Glaser, E. Mitochondrial targeting peptides in plants. *Trends Plant Sci.* **1998**, *3*, 136−140.
(16) Klaus, C.; Guiard, B.; Neupert, W.; Brunner, M. Determinants in the presequence of cytochrome b(2) for import into mitochondria and for proteolytic processing. *Eur. J. Biochem.* **1996**, *236*, 856−861.
(17) Chaumont, F.; de Castro Silva Filho, M.; Thomas, D.; Leterme, S.; Boutry, M. Truncated presequences of mitochondrial F1-ATPase β subunit from *Nicotiana plumbaginifolia* transport CAT and GUS proteins into mitochondria of transgenic tobacco. *Plant Mol. Biol.* **1994**, *24* (4), 631−641.
(18) von Heijne, G. Mitochondrial targeting sequences may form amphiphilic helices. *Embo J.* **1986**, *5*, 1335−1342.
(19) Chuah, J.-A.; Yoshizumi, T.; Kodama, Y.; Numata, K. Gene introduction into the mitochondria of *Arabidopsis thaliana* via peptide-based carriers. *Sci. Rep.* **2015**, *5* (1), 7751.
(20) Chuah, J. A.; Matsugami, A.; Hayashi, F.; Numata, K. Self-Assembled Peptide-Based System for Mitochondrial-Targeted Gene Delivery: Functional and Structural Insights. *Biomacromolecules* **2016**, *17*, 3547−3557.
(21) Yoshizumi, T.; Oikawa, K.; Chuah, J. A.; Kodama, Y.; Numata, K. Selective Gene Delivery for Integrating Exogenous DNA into Plastid and Mitochondrial Genomes Using Peptide-DNA Complexes. *Biomacromolecules* **2018**, *19*, 1582−1591.
(22) Yoshinaga, N.; Numata, K. Rational Designs at the Forefront of Mitochondria-Targeted Gene Delivery: Recent Progress and Future Perspectives. *ACS Biomater. Sci. Eng.* **2022**, *8*, 348−359.
(23) Abe, N.; Fujita, S.; Miyamoto, T.; Tsuchiya, K.; Numata, K. Plant Mitochondrial-Targeted Gene Delivery by Peptide/DNA Micelles Quantitatively Surface-Modified with Mitochondrial Targeting and Membrane-Penetrating Peptides. *Biomacromolecules* **2023**, *24*, 3657−3665.
(24) Law, S. S. Y.; Liou, G.; Nagai, Y.; Gimenez-Dejoz, J.; Tateishi, A.; Tsuchiya, K.; Kodama, Y.; Fujigaya, T.; Numata, K. Polymer-coated carbon nanotube hybrids with functional peptides for gene delivery into plant mitochondria. *Nat. Commun.* **2022**, *13* (1), 2417.
(25) Hurt, E. C.; Pesold-Hurt, B.; Suda, K.; Oppliger, W.; Schatz, G. The first twelve amino acids (less than half of the pre-sequence) of an imported mitochondrial protein can direct mouse cytosolic dihydrofolate reductase into the yeast mitochondrial matrix. *Embo J.* **1985**, *4*, 2061−2068.
(26) Maarse, A. C.; Van Loon, A. P.; Riezman, H.; Gregor, I.; Schatz, G.; Grivell, L. A. Subunit IV of yeast cytochrome c oxidase: Cloning and nucleotide sequencing of the gene and partial amino acid sequencing of the mature protein. *Embo J.* **1984**, *3*, 2831−2837.
(27) Hamasaki, H.; Yoshizumi, T.; Takahashi, N.; Higuchi, M.; Kuromori, T.; Imura, Y.; Shimada, H.; Matsui, M. SD3, an *Arabidopsis thaliana* homolog of TIM21, affects intracellular ATP levels and seedling development. *Mol. Plant* **2012**, *5*, 461−471.
(28) Cheng, M. Y.; Hartl, F.-U.; Martin, J.; Pollock, R. A.; Kalousek, F.; Neuper, W.; Hallberg, E. M.; Hallberg, R. L.; Horwich, A. L. Mitochondrial Heat-Shock Protein Hsp60 Is Essential for Assembly of Proteins Imported into Yeast Mitochondria. *Nature* **1989**, *337* (6208), 620−625.
(29) Almagro Armenteros, J. J.; Salvatore, M.; Emanuelsson, O.; Winther, O.; von Heijne, G.; Elofsson, A.; Nielsen, H. Detecting sequence signals in targeting peptides using deep learning. *Life Sci. Alliance* **2019**, *2*, No. e201900429.
(30) Doniwa, Y.; Arimura, S.; Tsutsumi, N. Mitochondria use actin filaments as rails for fast translocation in Arabidopsis and tobacco cells. *Plant Biotechnol.* **2007**, *24*, 441−447.
(31) Notredame, C.; Higgins, D. G.; Heringa, J. T-Coffee: A novel method for fast and accurate multiple sequence alignment. *J. Mol. Biol.* **2000**, *302*, 205−217.
(32) Taly, J. F.; Magis, C.; Bussotti, G.; Chang, J. M.; Di Tommaso, P.; Erb, I.; Espinosa-Carrasco, J.; Kemena, C.; Notredame, C. Using the T-Coffee package to build multiple sequence alignments of protein, RNA, DNA sequences and 3D structures. *Nat. Protoc.* **2011**, *6*, 1669−1682.
(33) Lithgow, T. Targeting of proteins to mitochondria. *FEBS Lett.* **2000**, *476*, 22−26.
(34) Abramson, J.; Adler, J.; Dunger, J.; Evans, R.; Green, T.; Pritzel, A.; Ronneberger, O.; Willmore, L.; Ballard, A. J.; Bambrick, J. Accurate structure prediction of biomolecular interactions with AlphaFold 3. *Nature* **2024**, *630*, 493−500.
(35) Terada, K.; Gimenez-Dejoz, J.; Kurita, T.; Oikawa, K.; Uji, H.; Tsuchiya, K.; Numata, K. Synthetic Mitochondria-Targeting Peptides Incorporating alpha-Aminoisobutyric Acid with a Stable Amphiphilic Helix Conformation in Plant Cells. *ACS Biomater. Sci. Eng.* **2021**, *7*, 1475−1484.
(36) Numata, K.; Horii, Y.; Oikawa, K.; Miyagi, Y.; Demura, T.; Ohtani, M. Library screening of cell-penetrating peptide for BY-2 cells, leaves of Arabidopsis, tobacco, tomato, poplar, and rice callus. *Sci. Rep.* **2018**, *8* (1), 10966.
(37) Ma, J. F.; Yamaji, N. Silicon uptake and accumulation in higher plants. *Trends Plant Sci.* **2006**, *11*, 392−397.
(38) Maliga, P.; Tungsuchat-Huang, T. Plastid transformation in *Nicotiana tabacum* and Nicotiana sylvestris by biolistic DNA delivery to leaves. *Methods Mol. Biol.* **2014**, *1132*, 147−163.
(39) Bolte, S.; Cordelieres, F. P. A guided tour into subcellular colocalization analysis in light microscopy. *J. Microsc.* **2006**, *224*, 213−232.
(40) Madeira, F.; Pearce, M.; Tivey, A. R. N.; Basutkar, P.; Lee, J.; Edbali, O.; Madhusoodanan, N.; Kolesnikov, A.; Lopez, R. Search and sequence analysis tools services from EMBL-EBI in 2022. *Nucleic Acids Res.* **2022**, *50*, W276−W279.

https://doi.org/10.1021/acschembio.4c00625
ACS Chem. Biol. 2024, 19, 2515−2524